Journal of Engineering Science and Technology
Vol. 16, No. 2 (2021) 1561 - 1576

ENHANCING EFFECTIVENESS OF GRID-CONNECTED PHOTOVOLTAIC SYSTEMS BY USING HYBRID ENERGY STORAGE SYSTEMS

HONG VIET PHUONG NGUYEN*, VAN TAN NGUYEN, QUANG SON VO, BINH NAM NGUYEN, HUU DAN DAO, DINH MINH DUC TRUONG

Faculty of Electrical Engineering, University of Science and Technology - The University of Danang, 54 Nguyen Luong Bang Street, Danang, Vietnam
*Corresponding Author: nhvphuong@dut.udn.vn

Abstract

This research presents a suggestion to improve the efficiency of grid-connected photovoltaic system by integrating hybrid energy storage sources. They are used to improve the quality of output power from the photovoltaic system. The variation of output power depends heavily on weather conditions, leading to adversely affect the power system's stability to which they are linked. This model is built in Matlab/Simulink environment by utilizing mathematical models. The simulation results show that this hybrid model helps photovoltaic system becoming a dispatchable power source which can quickly meet the power requirements of the grid thanks to the utilization of battery-supercapacitor based system. Moreover, the system can operate in the smoothing mode of the output power from the photovoltaic system when only supercapacitor is used. The control scheme of this hybrid system is successfully demonstrated to guarantee the quality and stability of the power system integrated with renewable sources. This model is essential for photovoltaic systems, especially when they are connected to a poor grid.

Keywords: Battery, Dispatchable generator, Grid-connected mode, Photovoltaic system, Supercapacitor.

1. Introduction

The continuously enormous increase of renewable energy sources in power system has facilitated great concerns about energy issues, especially from solar energy sources [1]. Power plants with large rotating inertia such as hydro power and thermal power mainly use synchronous generators (SG) which can easily support power system stability due to inherent rotating inertia of the generator's rotor and its damping characteristics. Nevertheless, for the converter-based photovoltaic (PV) sources which are low inertia sources due to their dependence on natural conditions, PV systems are considered as non-dispatchable power plants. Consequently, even small disturbances can likely affect the power system stability when the penetration rate of these sources in the power system increases, and thus this makes the power quality greatly affected [2]. Miñambres-Marcos et al. [3] and Altin [4] proposed the use of energy storage system (ESS) in PV systems to form a hybrid system (HS) to overcome this problem. Via appropriate control strategies, ESS can help the PV systems becoming more flexible, dispatchable, and meeting quickly power requirements when the power grid needs to be mobilized for regulating the power system's frequency. ESS is greatly helpful in improving the power quality of the system integrated with large renewable energy sources. They quickly respond to electric power needs by increasing or decreasing capacity instantly, therefore enhancing the output power of PV systems.

The PV system's output power is continuously varied, resulting in continuous charging/discharging of the energy storage system, so supercapacitor (SC) is used together with batteries to form a hybrid energy storage system (HESS) to protect their life cycles when chemical reactions happen within the battery. Although the energy density in SC is lower than in battery, SC are very useful in supporting for battery with slow response frequency when the power grid needs to mobilize power quickly to meet the users' demands due to their quick response capability [5].

In the recent years, HESS systems have gradually become important applications to stabilize power systems with the integration of major renewable energy sources. Therefore, different models and control schemes of HESS have been presented to investigate this matter. Kollimalla et al. [6] suggested a control scheme for sharing power between SC and battery. This introduced control strategy regulates the DC bus voltage for any power mismatch between PV and load demand. Jiang et al. [7] and Ma et al. [8] proposed control strategies for HESS to smooth the fluctuations of PV generated power. Kollimalla et al. [9] presented a control proposed through decoupling of different frequency power components. Chen et al. [10] showed the hierarchical optimal operation strategy for HESS which is suitable to be utilized in distribution grid with high penetration of PV to achieve PV power smoothing, voltage regulation and price arbitrage. Kotra and Mishra [11] and Kumar et al. [12] also addressed the energy management strategies of HESS to operate optimally and limit the state of charge of storage sources. In aforementioned research, the focuses were about control strategies and energy management algorithms. However, an adaptive control strategy for HESS operation under various conditions has not been studied. In this research, a comprehensive control scheme of HESS which can operate in both dispatchable and smoothing modes of PV output power is proposed. Thus, it can provide the rightful informative applications in industrial as well as future research on related topics.

This paper investigates a grid-connected renewable system with the main source of photovoltaic system supported by the HESS storage system. The system could be

operated in either dispatchable or power smoothing mode. In normal operation, the system is responsible for smoothing the PV output power. When the reference generated power is changed due to the load variation in the grid, the control system quickly switches to dispatchable mode. The whole control model is established from the mathematical and average models of converters. The paper presents comprehensive control diagram of the whole system, which is analysed, modelled, and simulated to outstanding the true behaviour of the system. The rest of the paper is organised as follows. Section 2 of this paper presents the general arrangement of the studied model. Next, section 3 presents proposed schemes and control strategies. Section 4 presents preliminary computation of supercapacitor and battery capacity. Section 5 provides simulation results in Matlab/Simulink software. Finally, Section 6 concludes this research.

2. General Structure of Studied Model

The general structure of the PV system integrated with the battery/supercapacitor-based energy storage system is illustrated in Fig. 1 in the grid-connected mode. The hybrid system including PV and HESS operates in two modes: dispatchable mode and power output smoothing mode. The power output from PV arrays is injected to the DC bus via a DC/DC boost converter. This boost device is equipped with a maximum power point tracking (MPPT) function to act as an MPPT controller for PV arrays when the P-V curve of the solar panels changes according to solar irradiance during daytime [13-15]. The energy storage system including a battery bank and a supercapacitor is linked to the DC bus through a bidirectional DC/DC converter [16] that has a control function to mitigate the power difference between the output from PV systems and the requirement from the grid in dispatchable mode.

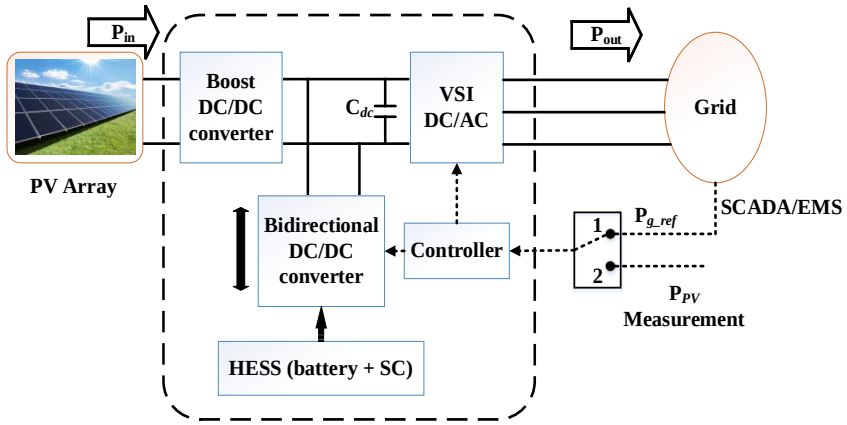

Fig. 1. Structure of hybrid system including PV and HESS.

When the PV output is larger than the power required from the power grid, the storage system operates in charging mode. On the other hand, the PV output power is smaller than the power required from the power grid, the energy storage system operates in discharging mode. In smoothing mode, HESS is utilized to smooth the power output of PV for reducing the grid's negative impacts. A voltage-source inverter (VSI) is employed to connect the DC bus to the power grid. It is also responsible for injecting active and reactive power to the power grid and stabilizing

the voltage of the DC bus connected to the capacitor C_{dc} [17, 18]. The controller block processes signals received from the power grid (mode 1) through SCADA/EMS system or the measured PV power (mode 2) and sends control pulses to power electronic devices to manipulate the power flown through the inverter.

3. System Control Strategies

The control scheme of the whole system includes two main parts: the control of the VSI and the governor of the battery/supercapacitor-based storage system. Details of these controllers are presented in the following parts.

3.1. Control scheme of voltage-source inverter

In grid-connected mode, the VSI controls the total power flow generated by the solar arrays and energy storage systems to grid and simultaneously stabilize the voltage of the capacitor C_{dc} of the DC bus as presented in Fig. 2 [17, 18]. As can be seen in Fig. 2, the reference active power, P_{g_ref}, is given from the V_{dc} voltage controller. Meanwhile, the reference reactive power, Q_{g_ref}, is controlled separately. Normally, Q_{g_ref} is controlled at zero value for VSI to operate at unity power factor. In other cases, Q_{g_ref} is controlled in order to stabilize the voltage of the AC bus. Figure 3 depicts the V_{dc} voltage control loop diagram in which the term V_{dc}^2 is controlled as it is comparative to the energy stored in the capacitor C_{dc}. The voltage of the capacitor C_{dc} is stabilized by maintaining the energy balance through the Eq. (1) (assuming VSI losses are ignored) [19]:

$$P_{sum} = P_{dc} + P_g \tag{1}$$

where P_{sum} is the total power generated by PV and HESS; P_{dc} is the power exchanged with capacitor C_{dc} and P_g is the power flown to the power grid.

When the voltage of the DC bus capacitor is maintained stably, the value of P_{dc} is zero, from Eq. (1) it can be derived:

$$P_{sum} = P_g \tag{2}$$

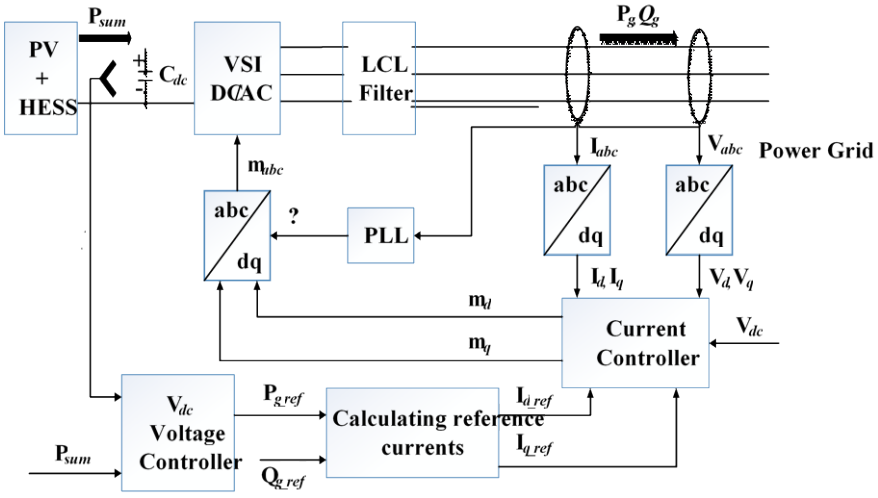

Fig. 2. Control structure of VSI in grid-connected mode.

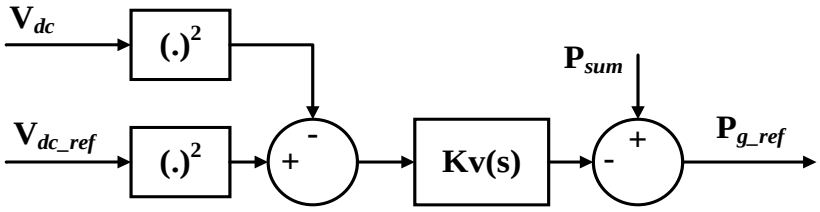

Fig. 3. Control scheme of DC bus voltage.

Equation (2) indicates that the power flown to the grid P_g is transferred through the VSI to inject the total power P_{sum} from the DC bus to grid. This value P_{sum} can be generated by utilizing the combination of battery/SC-based storage sources as outlined in Section 3.2. Next, the reference currents (I_{d_ref}, I_{q_ref}) are determined from reference power values and then fed to the current controller. The I_{d_ref} and I_{q_ref} are calculated by [18]:

$$I_{d\_ref} = \frac{2P_{g\_ref}}{3V_d} \tag{3}$$

$$I_{q\_ref} = \frac{-2Q_{g\_ref}}{3V_d} \tag{4}$$

The current controller, known as the current decoupled controller, aims to control the real and imaginary power independently of each other. The I_{d_ref} component controls the real power, while I_{q_ref} manages the imaginary power. After calculating the modulation indices m_d and m_q from the current controller, a converter block is used to change these indices from the *dq* frame to the *abc* three-phase frame through Park's matrix transformation [18]. Then, m_{abc} signal is sent to the VSI averaged model to control active and reactive powers to the reference values. The phase-lock loop (PLL) shown in Fig. 2 is used to synchronize powers with the grid and give reference phase angle values to the conversion block of *abc* to *dq* frame or vice versa [18].

Current control loop using PI controllers is determined by:

$$V_{td} = V_d - \omega L I_q + (I_{d\_ref} - I_d)\left(k_p + \frac{k_i}{s}\right) \tag{5}$$

$$V_{tq} = V_q + \omega L I_d + (I_{q\_ref} - I_q)\left(k_p + \frac{k_i}{s}\right) \tag{6}$$

where V_{td} and V_{tq} are *d*-axis and *q*-axis are VSI terminal voltage components correspondingly; V_d and V_q are *d*-axis and *q*-axis are voltage components of grid respectively; I_{d_ref} and I_{q_ref} are reference components of the current flowing through filter of VSI; I_d and I_q are actual current components flowing through filter of VSI; ω is grid angular frequency and k_p, k_i are factors of PI controller.

3.2. Control scheme of the hybrid energy storage system

The overall control scheme of HESS is illustrated as in Fig. 4. PV-HESS system operates in two modes: dispatchable and smoothing mode. In the former mode, the power difference between the PV output and the grid's required power is calculated and gives the reference value P_{HESS_ref} to the HESS controller. As the SC responds

faster than battery when power variation suddenly happens in a very short time, it is used to quickly compensate for sudden power changes [20, 21]. Battery with higher energy density is used for long-term energy storage due to its slower response. By default, the PV-HESS is in the power output smoothing mode to smooth out the PV power fluctuations and hence, suppress them from transferring to the power grid that can adversely affect the power quality of grid. Therefore, the power of the SC needs to be regulated to compensate power for the PV power fluctuations. To accomplish this goal, the reference power P_{SC_ref} can be determined by employing the averaging block as illustrated in Fig. 4. The power injected to the common DC bus from the PV array is measured and passed through an averaging mechanism with a fundamental frequency fc. Then, the filtered signal is subtracted by the corresponding original measured signal and result output is used as P_{SC_ref}. The value P_{SC_ref} is sent to the SC controller to generate duty cycle. In this smoothing mode, only SC storage source is sufficient, so battery is not required to be operated.

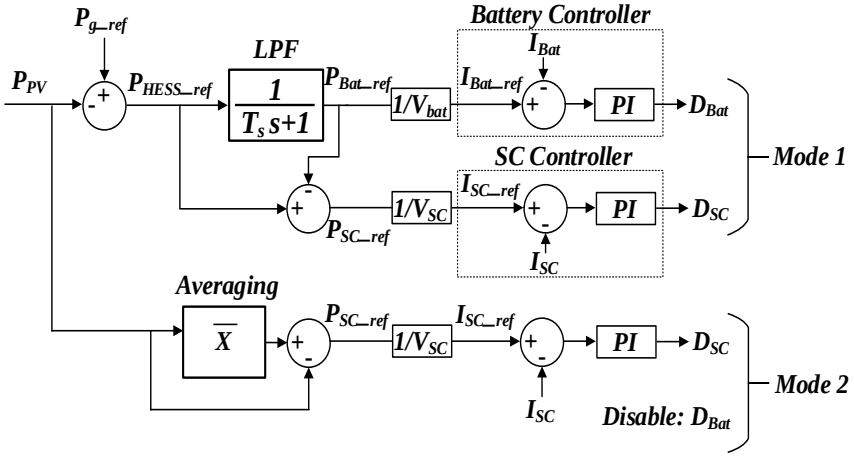

Fig. 4. Proposed control scheme of HESS.

3.3. Power sharing control in HESS in dispatchable mode

The flowchart of managing the power from the HESS is presented in Fig. 5. The power discrepancy between the PV output and the grid's required power is calculated and gives the reference value PHESS to the HESS controller. The controller can operate in two states: discharging state where the power is transmitted from storage sources to the DC bus and charging state where the storage sources is charged from the DC bus [22-26].

A low pass filter shown in Fig. 6 is designed with time constant, T_s, to acquire the variable power P_{batt_ref} and send to the battery controller. The remaining power that is highly variable power P_{sc_ref} is sent to the SC controller [19].

The detailed scheme of the battery and SC controllers is shown in Fig. 7. These controllers employ the approach of controlling the current via PI controllers. The duty cycle D of the controller is sent to DC/DC converters. These bidirectional converters can operate in two modes: discharge state where the power is transmitted from storage sources to the DC bus and charging state where the power is charged from the DC bus to the storage sources [20-24].

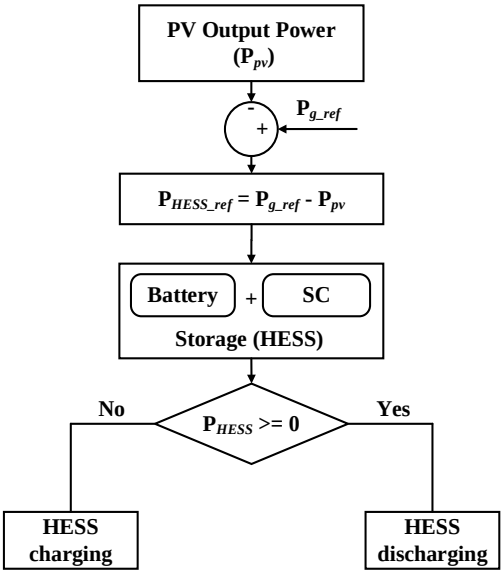

Fig. 5. Proposed control scheme of HESS.

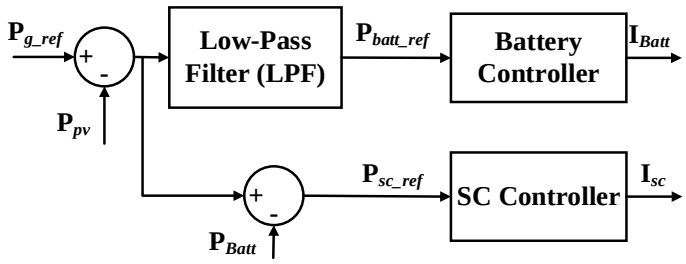

Fig. 6. Power sharing between battery and SC.

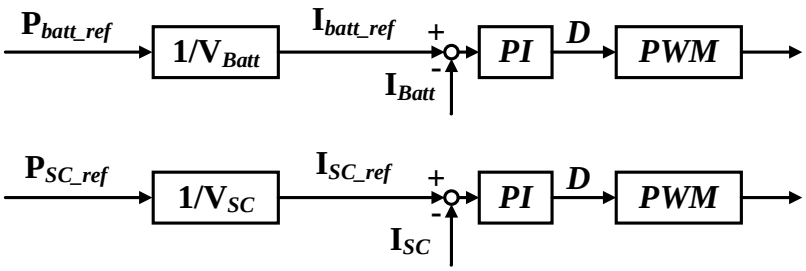

Fig. 7. Current control scheme of energy storage system.

4. Supercapacitor and Battery Bank Capacity Determination

4.1 Calculation of supercapacitor's capacity

In this research, capacity of supercapacitor is calculated in the worst case that it can respond enough energy on transient during time response period *t(s).*

The Eq. (7) for calculating the SC capacity is as follows [26]:

$$C_{sc} = \frac{2\Delta E_{sc}}{V_{scmax}^2 - V_{scmin}^2} \tag{7}$$

where V_{scmax} and V_{scmin} are the maximum and minimum values of safe operating voltage of SC, respectively. For efficiency and security reasons, the energy level must be limited from 25% to 95%. It corresponds to an operating voltage from 50% to 97.5%V_{scnom}. With the nominal voltage of SC system is V_{scnom} = 600V then according to [19]:

$$V_{scmin} = 50\%.V_{scnom} = 50\%.600 = 300\,V \tag{8}$$

$$V_{scmax} = 97.5\%.V_{scnom} = 97.5\%.600 = 585\,V \tag{9}$$

$$\Delta E_{sc} = P_{max}.t \tag{10}$$

where ΔE_{sc} is the energy deviation between the two states during the time period t(s).

It should be noticed that P_{max} is taken for the worst scenario when PV loses total power. Here, PV power used in this research is $P_{pv} = P_{max}$ = 2 MW. From Eq. (7), with response time of SC is equal to 0.7 s, it can be calculated that the value of C_{sc} as following:

$$C_{sc} = \frac{2|\Delta E|}{V_{sc\max}^2 - V_{sc\min}^2} = \frac{2 * P_{\max} * t(s)}{V_{sc\max}^2 - V_{sc\min}^2} = \frac{2*2*10^6*0.7}{585^2 - 300^2} = 11.1\ \text{F} \tag{11}$$

4.2 Calculation of battery's capacity

This article presents a simple way to calculate the storage capacity which can respond to the system demand within 1 hour. The battery's capacity is based on the generated energy of the renewable energy sources. It must be equal the amount of electricity produced in 1 hour of renewable energy sources.

The battery capacity is calculated by:

$$C_{bat} = \frac{P_{\max}.t_{\max}}{\eta.V_{batnom}} \tag{12}$$

where C_{bat} is the capacity of battery storage system, P_{max} and t_{max} are the maximum power of renewable energy sources and the insurance time, respectively. η is the charge/discharge efficiency of the battery energy storage system. For Lithium-ion batteries, this coefficient is used as $\eta = 0.9$ [27]. V_{batnom} is the rated voltage of battery system.

From Eq. (12), the capacity of battery bank is:

$$C_{bat} = \frac{2*10^6*1}{0.9*600} = 3703(\text{Ah}) \tag{13}$$

5. Simulation Results

This investigation aims to integrate the HESS (battery bank and SC) into PV system in grid-connected mode, together with power electronic converters to form the hybrid system (PV and HESS). As a result, the HESS system not only helps to reduce the power output fluctuations from PV system in normal operation mode

but also helps PV system to become a dispatchable source responding quickly to the power changes in the power grid. In this simulation, the boost converter which is linked to the solar arrays is regulated to trace the maximum power point. The VSI output is connected to the primary side of the step-up transformer. The entire model is built in Matlab/Simulink. Main parameters used to simulate the system are tabulated in Table 1.

able 1. Simulation parameters of studied system.

Description	Simulation parameter	
	Symbol	**Value**
Peak power of PV system	P_{pv}	2 MWp
Rated capacity of battery system	C_{bat}	3703 Ah
Rated voltage of battery system	V_{batnom}	600 V
Nominal capacity of SC system	C_{sc}	11.1 F
Nominal voltage of SC system	V_{scnom}	600 V
VSI filter resistance	R_f	0.75 mΩ
VSI filter reactance	L_f	100 μH
Capacitance of DC bus capacitor	C_{dc}	0.2 F
Nominal voltage of DC bus	V_{dcref}	1000 V
Nominal phase to phase voltage of grid	V_g	400 V
Nominal frequency of grid	f	50 Hz
Factors of PI controller of VSI	k_p, k_i	0.031; 0.5094
Time constant of Low – pass Filter	T_s	0.7

The data of solar irradiance in this simulation is depicted in Fig. 8(a). The output of the PV arrays is regulated to track the maximum power point according to the P&O algorithm [8] as illustrated in Fig. 8(b). It should be noticed from Fig. 8(a) that there is a sharp decrease of solar irradiance from near 1000 W/m^2 to near 200 W/m^2 at t = 52 s. This makes PV power output decrease suddenly at same time as in Fig. 8(b). This scenario is used in this simulation for both dispatchable and smoothing modes. As well-known, renewable energy sources such as PV must be able to maintain the active power generation under the free power generation mode and the generating power control mode. In generating power control mode, if the variation of primary energy source is equal to or greater than limit value according to dispatch command, it should generate the active power at the correct limit value according to dispatch command. In this case, assuming the PV-HESS is injected power to the power system to meet the active power demand shown in Fig. 9.

Simulation results of the power produced by the allocation between battery and SC are shown in Fig. 10. At t = 30 s, the grid power requirement decreases from 1.5 MW to 0.8 MW (see Fig. 9), currently the HESS storage system quickly operates in charging state. The SC receives large power charge in a very short time interval to ensure the system stability. As depicted in Fig. 10, the SC rate of power change is approximately 2.52 MW/s. At t = 52s, PV system's output power drops sharply from 2 MW to 0.2 MW to simulate for the partial shading scenario that usually occurs in PV systems while the required power of grid does not change at this moment. As a result, the SC's rate of discharge power is approximately 0.88 MW/s. At t = 70s, the required power of grid increases sharply from 0.62 MW to 1.5 MW while the PV power output is maintained steadily, the SC is controlled to inject the deficient generating power to the grid with the rate of power change about 2.11 MW/s. At all these moments, battery bank with a large energy density is used

to sustain long-term system power, thereby it can help to save costs and appropriately comply with the operation of the SC system.

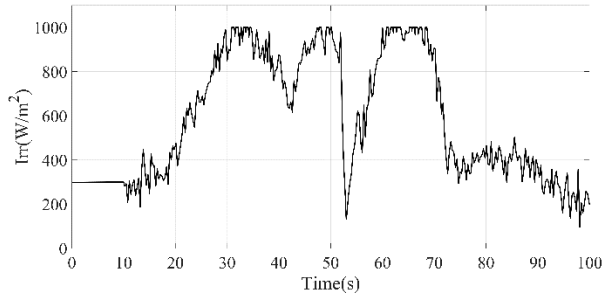

(a) Solar irradiance data

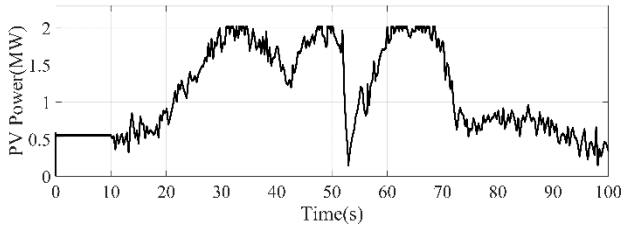

(b) PV system output power

Fig. 8. Solar irradiance data and PV system output power.

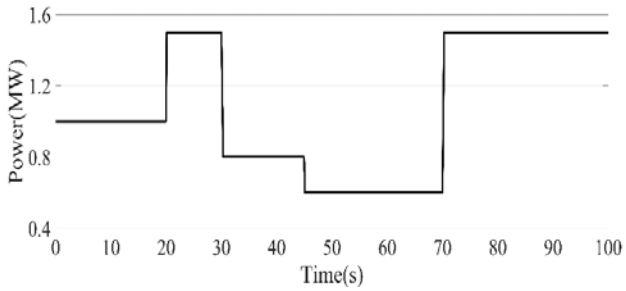

Fig. 9. Power required from the grid.

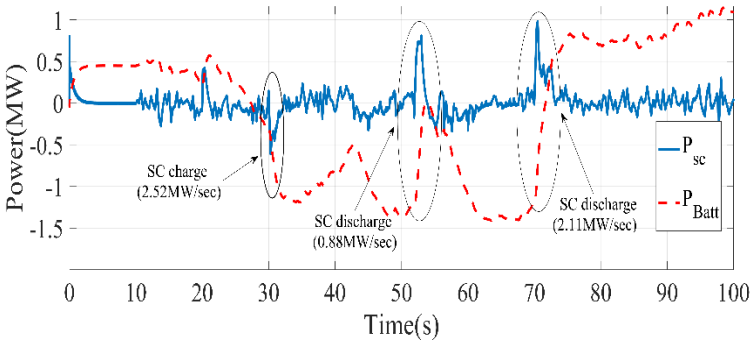

Fig. 10. Power of HESS injected into power grid.

The response time of SC and battery is shown as in Fig. 11. The SC with high power density responds to changes in the system immediately and battery with high energy density provides power in a long duration. From Fig. 11, SC responds rapidly within 0.45 s while battery only responds for the long-term power variations, so battery is responsible for injecting the base power into power system. In other words, the battery is utilized to balance the power difference between the PV-HESS and the power demand of power grid in steady-state.

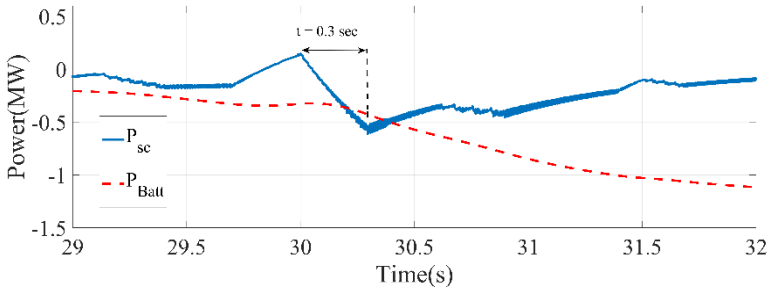

(a) At time *t* = 30 s.

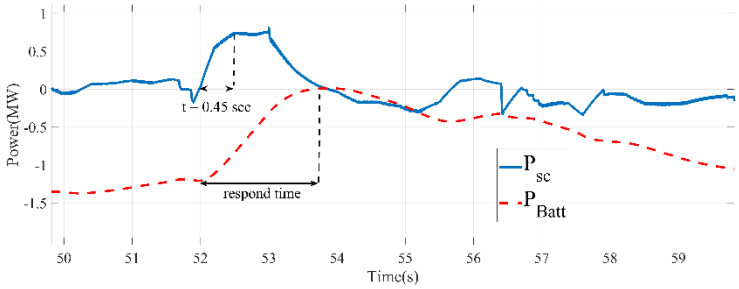

(b) At time *t* = 52 s.

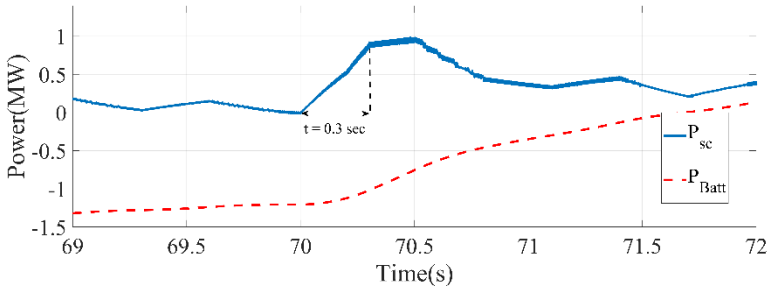

(c) At time *t* = 70 s.

Fig. 11. Comparison of capacity response between battery and SC.

Figure 12 shows the output power of the PV and HESS hybrid system controlled via the VSI against the reference power value required by the power grid as shown in Fig. 9. Simulation result shows that the controller operates effectively, helping the output power of the system to follow its reference value properly.

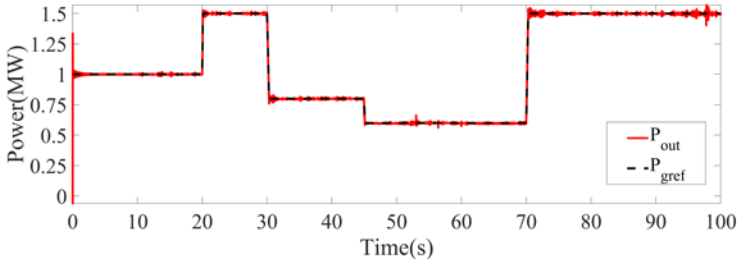

Fig. 12. Comparison of output of hybrid system and power required from the grid.

The fluctuation of DC bus voltage waveform is shown in Fig. 13. As the required power of grid changes, the grid frequency fluctuates consequently. Correspondingly, the DC bus voltage also fluctuates. When the required power increases, the grid frequency decreases, this causes a drop in the DC bus voltage and SC is in the state of discharge. On the other hand, the frequency increases while the required power decreases, causing the increase of the DC voltage and SC is in the state of charge. The voltage of the DC bus V_{dc} is controlled via VSI to be stabilized at reference value of 1000 V regardless of the output fluctuation of the PV arrays and the power required from the grid. Thanks to the controller $K_v(s)$, the DC bus voltage slightly fluctuates in extremely small range (less than 0.1 V in the worst case) as can be seen in Fig. 13.

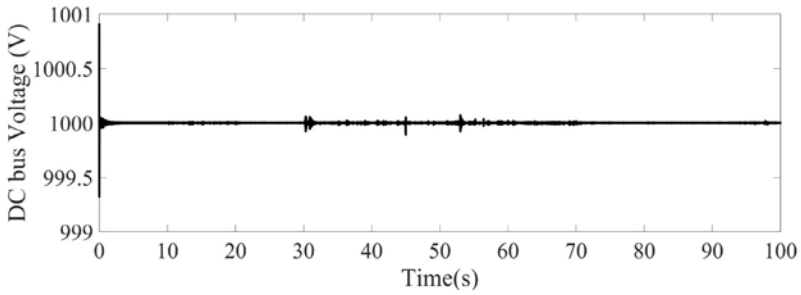

Fig. 13. DC bus voltage.

As mentioned above, PV also must be able to maintain the active power generation under the free power generation mode. In this case, the PV operates the maximum possible power 1according to the variation of the primary energy source. During the operation of the PV system, the switching capability from grid-following control mode to output power smoothing mode is essential to flatten the generated power from PV. The output power of PV-HESS system in this latter mode is shown in Fig. 14. In this mode, only SC is utilized to mitigate small fluctuations of the PV system. As the output power of the PV system is smoothed, the PV output power quality is enhanced in the normal operation mode, thereby improving power quality of the grid.

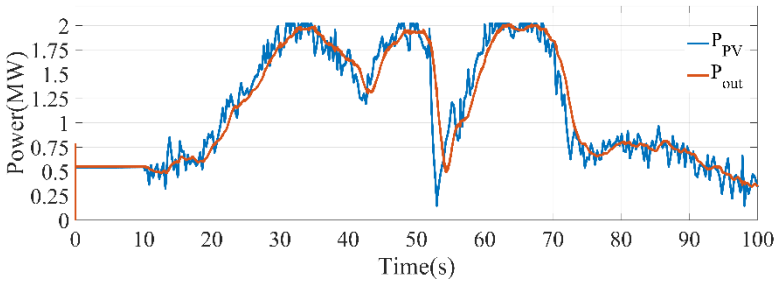

Fig. 14. Smoothing PV power mode.

6. Conclusions

In this paper, a control suggestion to ensure the power quality of the system incorporated with the battery/supercapacitor-based storage system is presented. The outcome of this approach is to form a dispatchable power source, meeting the power constraints of the grid regardless of the rapid power fluctuation of the PV system due to weather conditions in the generated power control mode.

Moreover, hybrid energy storage system also helps for PV system to reduce fluctuations in output power in normal mode. The employment of SC with fast charging/discharging capability in a short time interval is utilized for responding to sudden power fluctuations. Meanwhile, the battery storage system with long-term storage capability is utilized to maintain power stability. Simulation results show the effectiveness of the proposed control strategy of the hybrid energy storage system to transform the PV system into a flexible energy source in many cases. The study shows the importance of using battery/SC-based hybrid energy storage systems for distributed generation sources, especially for passive sources depending heavily on natural conditions such as solar and wind energy.

The outcome of this research also shows the promising capability of hybrid energy storage system in terms of system inertia support and primary frequency control. This could be the key feature for maintaining the stability of existing system's frequency. The supercapacitor is used to simulate the system inertia and deal with high frequency power fluctuations, whereas the battery bank is used to offset the power difference between the generations and demands.

Nomenclatures

C_{bat}	Nominal capacity of battery system, Ah
C_{dc}	Capacity of the DC-bus capacitor, F
C_{SC}	Nominal capacity of SC system, F
D	Duty cycle
I_{batt}	Current delivered by battery, A
I_{batt_ref}	Reference current of battery, A
I_{SC}	SC current, A
I_{SC_ref}	SC reference current, A
I_d	*d*-axis current flown through VSI filter, A
I_{d_ref}	*d*-axis reference current flown through VSI filter, A
I_q	*q*-axis current flown through VSI filter, A
I_{q_ref}	*q*-axis reference current flown through VSI filter, A

I_t	Calculated current of the load, A
k	Average charge/discharge current of the battery
k_i	Integral coefficient of PI controller
k_p	Proportional coefficient of PI controller
L	Reactance of VSI filter, H
m_{abc}	VSI three-phase modulation index
m_d	VSI *d*-axis modulation index
m_q	VSI *q*-axis modulation index
P_{batt_ref}	Reference power of battery system, kW
P_{dc}	Power exchanged with DC-bus capacitor, kW
P_{HESS}	Reference power of HESS system, kW
P_g	Required power of the power grid, MW
P_{g_ref}	Required reference active power of the power grid, MW
P_{max}	Maximum power used for calculating SC capacity, kW
P_{pv}	Output power of PV system, MW
P_{SC_ref}	Reference power of SC system, kW
P_{sum}	Total power generated by PV and HESS, MW
Q_{g_ref}	Required reference reactive power of the power grid, MVAr
T_s	Time constant of low-pass filter, s
t	Simulation time period, s
V_d	*d*-axis grid voltage component, V
V_{dc}	Voltage of DC-bus capacitor, V
V_q	*q*-axis grid voltage component, V
V_{SCmax}	Maximum value of safe operating voltage of SC, V
V_{SCmin}	Minimum value of safe operating voltage of SC, V
V_{SCnom}	Nominal voltage of SC system, V
V_{td}	*d*-axis component of VSI terminal voltage, V
V_{tq}	*q*-axis component of VSI terminal voltage, V
ΔE_{sc}	Energy deviation between the two states during the time period *t*, kWh

Greek Symbols

μ	Calculated current ratio of the load
ω	Angular frequency of power grid, rad/s

Abbreviations

HESS	Hybrid Energy Storage System
HS	Hybrid System
MPPT	Maximum Power Point Tracking
PI	Proportional Integral
P&O	Perturb & Observe
PLL	Phase Lock Loop
PV	Photovoltaic
SC	Supercapacitor
SG	Synchronous Generator
VSI	Voltage Source Inverter

Acknowledgements

This research is funded by Funds for Science and Technology Development of the University of Danang under project number B2019-DN02-57.

References

1. Masters, G.M. (2005). *Renewable and efficient electric power systems*. Canada: John Wiley and Sons Inc.
2. Tamrakar, U.; Shrestha, D.; Maharjan, M.; Bhattarai, B.P.; Hansen, T.M.; and Tonkoski, R. (2017). Virtual inertia: current trends and future directions. *Applied Sciences*, 7(7), 1-29.
3. Miñambres-Marcos, V.M.; Guerrero-Martínez, M.A.; Barrero-González, F.; and Milanés-Montero, M.I. (2017). A grid connected photovoltaic inverter with battery-supercapacitor hybrid energy storage. *Sensors*, 17(8), 1-8.
4. Altin, N. (2016). Energy storage systems and power system stability. *Proceedings of the 2016 International Smart Grid Workshop and Certificate Program (ISGWCP)*. Istanbul, Turkey, 1-7.
5. Wang, L.; Vo, Q.-S.; and Prokhorov, A.V. (2018). Stability improvement of a multimachine power system connected with a large-scale hybrid wind-photovoltaic farm using a supercapacitor. *IEEE Transactions on Industry Applications*, 54(1), 50-60.
6. Kollimalla, S.K.; Mishra, M.K.; and Narasamma, N.L. (2014). Design and analysis of novel control strategy for battery and supercapacitor storage system. *IEEE Transactions on Sustainable Energy*, 5(4), 1137-1144.
7. Jiang, W.; Zhang, L.; Zhao, H.; Huang, H.; and Hu, H. (2016). Research on power sharing strategy of hybrid energy storage system in photovoltaic power station based on multi-objective optimisation. *IET Renewable Power Generation*, 10(5), 575-583.
8. Ma, W.; Wang, W.; Wu, X.; Hu, R.; Tang, F.; and Zhang, W. (2019). Control strategy of a hybrid energy storage system to smooth photovoltaic power fluctuations considering photovoltaic output power curtailment. *Sustainability*, 11(5).
9. Kollimalla, S.K.; Mishra, M.K.; and Narasamma L.N. (2014). Coordinated control and energy management of hybrid energy storage system in PV system. *Proceedings of the 2014 International Conference on Computation of Power, Energy, Information and Communication (ICCPEIC)*. Chennai, India, 363-368.
10. Chen, J.; Li, J.; Zhang, Y.; Bao, G.; Ge, X.; and Li, P. (2018). A hierarchical optimal operation strategy of hybrid energy storage system in distribution networks with high photovoltaic penetration. *Energies*, 11(2).
11. Kotra, S.; and Mishra, M.K. (2017). A supervisory power management system for a hybrid microgrid with HESS. *IEEE Transactions on Industrial Electronics*, 64(5), 3640-3649.
12. Kumar, G.V.B.; Kaliannan, P.; Padmanaban, S.; Holm-Nielsen, J.B.; and Blaabjerg, F. (2020). Effective management system for solar PV using real-time data with hybrid energy storage system. *Applied Sciences*, 10(3).
13. Nguyen, B.N.; Pham, V.K.; Nguyen, V.T.; Hoang, D.H.; Truong, T.B.T.; and Nguyen, H.V.P. (2019). A new maximum power point tracking algorithm for the photovoltaic power system. *Proceedings of the 2019 International Conference on System Science and Engineering (ICSSE)*. Dong Hoi, Vietnam, 159-163.
14. Tan, N.V.; Nam, N.B.; Hieu, N.H.; Hung, L.K.; Duong, M.Q.; and Lam, L.H. (2020). A proposal for an MPPT algorithm based on the fluctuations of the PV

output power, output voltage, and control duty cycle for improving the performance of PV systems in microgrid. *Energies*, 13(17).

15. Nguyen, B.N.; Nguyen, V.T.; Duong, M.Q.; Le, K.H.; Nguyen, H.H.; and Doan, A.T. (2020). Propose a MPPT algorithm based on thevenin equivalent circuit for improving photovoltaic system operation. *Frontiers in Energy Research*, 8(14), 1-13.
16. Karshenas, H.R.; Daneshpajooh, H.; Safaee, A.; Jain, P.; and Bakhshai, A. (2011). *Energy storage in the emerging era of smart grid*. Chapter: Bidirectional DC - DC converters for energy storage systems. Croatia: InTech, 161-178.
17. Egea-Alvarez, A.; Junyent-Ferré, A.; and Gomis-Bellmunt, O. (2012). *Modeling and control of sustainable power systems*. Chapter: Active and reactive power control of grid connected distributed generation systems. Berlin: Springer, 47-81.
18. Yazdani, A.; and Iravani, R. (2010). *Voltage-sourced converters in power systems: modeling, control, and applications*. Canada: John Wiley and Sons.
19. Lu, D. (2011). *Design and control of a PV active generator with integrated energy storages: application to the aggregation of producers and consumers in an urban micro smart grid.* Doctoral dissertation, École Centrale de Lille, France.
20. Hajiaghasi, S.; Salemnia, A.; and Hamzeh, M. (2018). Hybrid energy storage for microgrid performance improvement under unbalanced load conditions. *Journal of Energy Management and Technology*, 2(1), 32-41.
21. Moghbelli, H.; and Sabzi, S. (2015*).* Analysis and simulation of hybrid electric energy storage (HEES) systems for high power applications. *Proceedings of the 122nd ASEE Annual Conference and Exposition*. Seattle, USA, 1-13.
22. Letting, L.K.; Mundaa, J.L.; and Hamam, Y. (2014). Dynamic performance analysis of an integrated wind-photovoltaic microgrid with storage. *International Journal of Smart Grid and Clean Energy*, 3(3), 307-317.
23. Jing, W.; Lai, C.H.; Wong, W.S.H.; and Wong, M.L.D. (2017). Dynamic power allocation of battery-supercapacitor hybrid energy storage for standalone PV microgrid applications. *Sustainable Energy Technologies and Assessments*, 22(7), 55-64.
24. Jayalakshmi, N.S.; Gaonkar, D.N.; Kumar, V.J.; and Karthik, R.P. (2015). Battery-ultracapacitor storage devices to mitigate power fluctuations for grid connected PV system. *Proceedings of the 2015 Annual IEEE India Conference (INDICON)*. New Delhi, India, 1-6.
25. Worku, M.Y. (2017). Power smoothing control of PMSG based wind generation using supercapacitor energy storage system. *International Journal of Emerging Electric Power Systems*, 18(4), 1-18.
26. Mendis, N.; Muttaqi, K.M.; and Perera, S. (2012). Active power management of a super capacitor-battery hybrid energy storage system for standalone operation of DFIG based wind turbines. *Proceedings of the 2012 IEEE Industry Applications Society Annual Meeting*. Las Vegas, USA, 1-8.
27. Akram, U.; Nadarajah, M.; Shah, R.; and Milano, F. (2020). A review on rapid responsive energy storage technologies for frequency regulation in modern power systems. *Renewable and Sustainable Energy Reviews*, 120.